Tantalum Oxide Thin Films Sputter-Deposited by Oxygen Gas Pulsing

Nicolas Martin *, Cote Jean-Marc , Gavoille Joseph , Potin Valerie

Posted Date: 17 October 2023

doi: 10.20944/preprints202310.1045.v1

Keywords: Tantalum oxide; thin film; reactive sputtering; gas pulsing; metal; semi-conductor; dielectric; periodic multilayers.

Article

Tantalum Oxide Thin Films Sputter-Deposited by Oxygen Gas Pulsing

Nicolas Martin [1,*], Jean-Marc Cote [1], Joseph Gavoille [1] and Valérie Potin [2]

[1] Institut FEMTO-ST, UMR 6174, CNRS, ENSMM, Univ. Bourgogne Franche-Comté, 15B, Avenue des Montboucons, 25030 BESANCON Cedex, France

[2] Laboratoire Interdisciplinaire Carnot de Bourgogne (ICB), UMR 6303, CNRS, Univ. Bourgogne Franche-Comté, 9, Avenue Alain Savary, BP 47 870, F-21078 DIJON Cedex, France

* Correspondence: nicolas.martin@femto-st.fr; Tel.: +33-363-08-2431

Abstract: Tantalum oxide thin films are deposited by DC reactive magnetron sputtering from a tantalum metallic target and oxygen as reactive gas. The reactive gas pulsing process (RGPP) is implemented to produce TaO_x compounds with tunable chemical compositions. The argon mass flow rate is maintained constant whereas that of the oxygen gas is pulsed during the deposition. A constant pulsing period T = 10 s is used and the introduction time of the oxygen gas, namely the t_{ON} injection time, is systematically changed from 0 to 100 % of the pulsing period T. As the t_{ON} injection time increases, the chemical composition of as-deposited TaO_x films is continuously changed from pure metallic tantalum to the over-stoichiometric Ta_2O_5 material. Analysis of the crystallographic structure by X-ray diffraction shows that the films adopt the body-centered cubic structure (metallic Ta) for the lowest t_{ON} injection time values (oxygen stoichiometry $x < 1.0$) and become amorphous for the longest t_{ON} injection times. It is shown that the t_{ON} injection time is a key parameter to produce either homogeneous tantalum oxides, or periodic Ta/TaO_x multilayers with alternations close to 3 nm. Similarly, optical transmittance spectra of the film/glass substrate system are recorded in the visible region and the electrical conductivity of the films is measured *vs.* temperature. Both exhibit a gradual evolution from metallic ($\sigma_{300K} = 8.17\times10^5$ S m^{-1} with a null optical transmittance in the visible range) to semi-conducting ($\sigma_{300K} = 1.97\times10^3$ S m^{-1} with a semi-transparent behavior) and finally to dielectric properties ($\sigma_{300K} < 10^{-5}$ S m^{-1} for interferential films) as a function of the oxygen concentration in the films.

Keywords: tantalum oxide; thin film; reactive sputtering; gas pulsing; metal; semi-conductor; dielectric; periodic multilayers.

1. Introduction

Over the last few decades, many investigations have been focused on the growth and fabrication of thin films based-on transition metal oxides [1,2]. These materials are particularly attractive for their great potential in electronic, magnetic, and optical applications. They have been studied and sometime integrated into various devices such as gas sensors [3], electrochromic systems [4] and catalysts [5] among others. Film behaviors are strongly influenced by the structure at the micro- and nanoscale, but they depend at first on the chemical composition, especially the oxygen content. As a result, playing with the metalloid concentration in metal oxide thin films appears as an attractive strategy for tuning many physico-chemical properties [6–8]. While some transition metal oxides have ever been deeply investigated due to a spontaneous formation or the ease of fabrication, others like tantalum oxides [9,10] have been less studied and their deposition as a thin solid film with tunable compositions still remains a challenging task.

Tantalum oxide compound has great technological interest, particularly because of its optical and electrical performances [11–13]. This kind of material has attracted huge attention in recent years due to its potential applications as a high refractive index compound in high-finesses mirrors [14], as anti-reflecting coatings for solar cells [15], as optical waveguides [16], and as a dielectric capacitor in

 doi:10.20944/preprints202310.1045.v1

high density dynamic random-access memories (DRAMs) [17–19]. Compared to silicon dioxide, which has a dielectric constant of 3.9, stoichiometric tantalum oxide Ta_2O_5 compounds can provide about 5 to 6 times increase in the capacitance density (dielectric constant of Ta_2O_5 is in-between 20-27). This can provide a high packing density in the next generations of DRAMs without reducing the thickness of the dielectric materials to unachievable values. Because of such technological attraction, tantalum oxide thin films have been grown by a large variety of deposition methods including anodization, room temperature oxidation, ion-assisted deposition, chemical vapor deposition (CVD) and physical vapor deposition (PVD) [20–25]. TaO_x films prepared by these different techniques showed widely disperse properties depending on the process parameters, temperature grown, post-annealing conditions, etc. However, the influence of the oxygen concentration on some characteristics of as-deposited films has insufficiently been investigated, especially for the film prepared by reactive sputtering [26]. It mainly comes from the difficulties to synthesize metal oxide compounds and so thin films based-on tantalum, with tuneable element concentrations, due to instabilities of the reactive process [27–29]. Such a drawback restrains the range of reachable chemical compositions and consequently the resulting properties.

The purpose of this paper is to show how a pulsing injection of the oxygen gas can extend the panel of the oxygen contents and thus the resulting properties of sputter-deposited TaO_x films. The role of the pulsing parameters (injection time of the oxygen gas, namely the t_{ON} injection time, into the deposition process) on the properties of the films is principally investigated. A systematic increase of this oxygen injection time leads to amorphous tantalum oxides corresponding to a vanishing of the columnar structure, and for the shortest t_{ON} injection times, to the growth of periodic and nanometric multilayers. Optical characteristics in the visible region show that TaO_x films prepared with short t_{ON} injection times are mainly absorbent, whereas a high oxygen supply tends to produce semi-transparent and interferential Ta_2O_5 compounds. The reverse evolution of oxygen and tantalum concentrations is observed *vs.* the t_{ON} injection time, and correlated with the evolution of the film electrical properties to become semi-conductors and finally insulators.

2. Materials and Methods

Deposition of tantalum oxide thin films was performed by dc reactive magnetron sputtering inside a 40 L stainless-steel homemade vacuum reactor. The reactor, equipped with a circular planar and water-cooled magnetron sputtering source, was evacuated with a turbomolecular pump backed by a mechanical pump to obtain an ultimate pressure of 10^{-6} Pa. The pumping speed was kept constant at S = 13 L s^{-1}. The tantalum target (purity 99.6 at. %, 50 mm diameter) was DC sputtered with a constant current density J_{Ta} = 51 A m^{-2} in a reactive atmosphere composed of argon and oxygen gases. Argon flow rate was maintained at 4.4 sccm corresponding to an argon partial pressure of 0.3 Pa. A home-made computer-controlled system, namely the reactive gas pulsing process (RGPP), was used to introduce oxygen gas *vs.* time according to a rectangular shape [30,31]. A constant pulsing period T = 10 s was applied. A maximum oxygen flow rate q_{O2Max} = 1.6 sccm was used whereas the minimum oxygen flow rate was set at q_{O2min}= 0 sccm. Then, t_{ON} and t_{OFF} times were inversely and systematically changed from t_{ON} = 0 to 10 s. The target-to-substrate distance was 65 mm. Substrates, introduced through a 1 L airlock, were glass and (100) silicon wafers. Before each run they were cleaned with acetone and alcohol, and the tantalum target was pre-sputtered in a pure argon atmosphere for five minutes before introducing oxygen, in order to remove the target surface contamination layer. Room temperature was used for all deposition and the deposition time was adjusted in order to obtain a thickness close to 500 nm (measured by a mechanical profilometer). The chemical composition of the films deposited on (100) silicon wafer was determined by electron probe microanalysis (EPMA). Observations of the film's cross-section were performed by scanning electron microscopy (SEM). Optical transmittance spectra of tantalum oxide coatings deposited on glass substrates were recorded from a Lambda 20 UV– visible Perkin- Elmer spectrophotometer. The crystallographic structure was investigated by X-ray diffraction (XRD) using monochromatic Co K_α radiation with a θ/2θ configuration. The electrical conductivity was measured *vs.* temperature using the van der Pauw's method in a temperature range from 293 to 543 K. The microstructural analysis

Preprints (www.preprints.org) | NOT PEER-REVIEWED | Posted: 17 October 2023 doi:10.20944/preprints202310.1045.v1

was also carried out with a JEOL JEM 2100F Transmission Electron Microscope (TEM) operating at 200 keV. Cross-sections for TEM were prepared using the standard sandwich technique. They were mechanically polished, dimpled down to a thickness of 10 μm and Ar^+ ion milled to electron transparency. The TEM images were analyzed using the GATAN Digital Micrograph software whereas their simulations were obtained with the Java Electron Microscopy Software (JEMS). The chemical composition was also measured by energy-dispersive X-ray spectroscopy implemented in the TEM.

3. Results

3.1. Composition and structure

The deposition rate of TaO_x films is first determined as function of the t_{ON} injection time from the film's thickness measured by a mechanical profilometer (500 nm as a target) and knowing the deposition time (Figure 1).

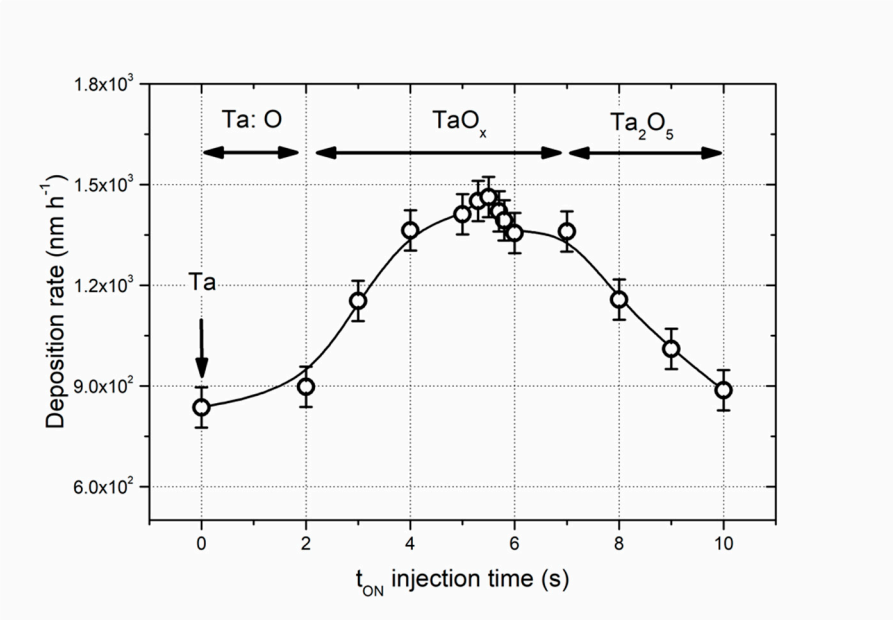

Figure 1. Influence of t_{ON} injection time on the TaO_x deposition rate. The oxygen mass flow rate is pulsed with a constant period T = 10 s. Deposition rate gradually changes and exhibits a maximum for t_{ON} close to 5 s. Three zones, namely Ta:O, TaO_x, and Ta_2O_5-like compounds, are suggested as a function of the t_{ON} injection time.

No abrupt drops of the deposition rate are obtained for a given supply of the oxygen gas, as commonly observed for transition metal oxide thin films sputter-deposited by the conventional reactive process (constant mass flow rate) [32]. A smooth and continuous evolution is rather produced when increasing the t_{ON} injection time. Without oxygen, pure metallic Ta films are prepared with a deposition rate of 840 nm h^{-1}. Injecting the oxygen gas with t_{ON} injection times of a few seconds leads to a significant increase of the deposition rate. The latter reaches a maximum value of 1460 nm h^{-1} in-between t_{ON} = 4-6 s. A further increase of the t_{ON} injection time reduces the rate , which goes down to 900 nm h^{-1} for a constant supply of oxygen (i.e., t_{ON} = 10 s). This continuous variation of deposition rate *vs.* t_{ON} injection time with an optimized condition is often obtained for oxides [33] and nitrides [34] prepared by reactive sputtering implementing RGPP. However, most of these ceramic thin films (e.g., TiO_2, ZrO_2, V_2O_5 …) exhibit a much lower deposition rate than those of the corresponding metal when the metallic target completely works in the poisoned sputtering mode (t_{ON} injection time tending to the pulsing period T). A few nanometers thick compound layer (oxide for reactive sputtering with O_2, and nitride with N_2) is formed on the target surface with a low sputtering yield, which reduces the deposition rate compared to that of metal. For reactive sputtering of

Preprints (www.preprints.org) | NOT PEER-REVIEWED | Posted: 17 October 2023 doi:10.20944/preprints202310.1045.v1

tantalum oxides (and also similarly reported for tungsten oxides [35]), rates corresponding to the deposition of the most stable and nearly stoichiometric compound (i.e., Ta_2O_5 in this study) is high or close to the same order of magnitude as the metallic one. Based-on former investigations proposed by Oechsner *et al.*, Ta_2O_5 is a particular compound for which its sputtering yield can be higher than that of the clean metal [36]. According to the same authors, this unusual behavior of Ta_2O_5 (also expected for tungsten and niobium oxides) gives rise to the sputtering of TaO and Ta neutral species as well as ionic, neutral and molecular oxygen. It is worth of noting that this high deposition rate of tantalum oxides is also connected to a balance between sputtering yield, kinetics of poisoning of the target surface, oxygen concentration and density of the deposited oxide, as previously reported for WO_x thin films [35].

Assuming the t_{ON} injection time as a key parameter for producing TaO_x films with various compositions, one may suggest three zones in Figure 1 corresponding to the deposition of Ta:O films for the very short t_{ON} injection times (lower than about 2 s), and amorphous a-Ta_2O_5-like film for the longest ones (higher than about 6 s). Between these two t_{ON} injection times, TaO_x compounds can be prepared. This adjustable films composition is well illustrated plotting the tantalum and oxygen concentrations as a function of the t_{ON} injection time (Figure 2).

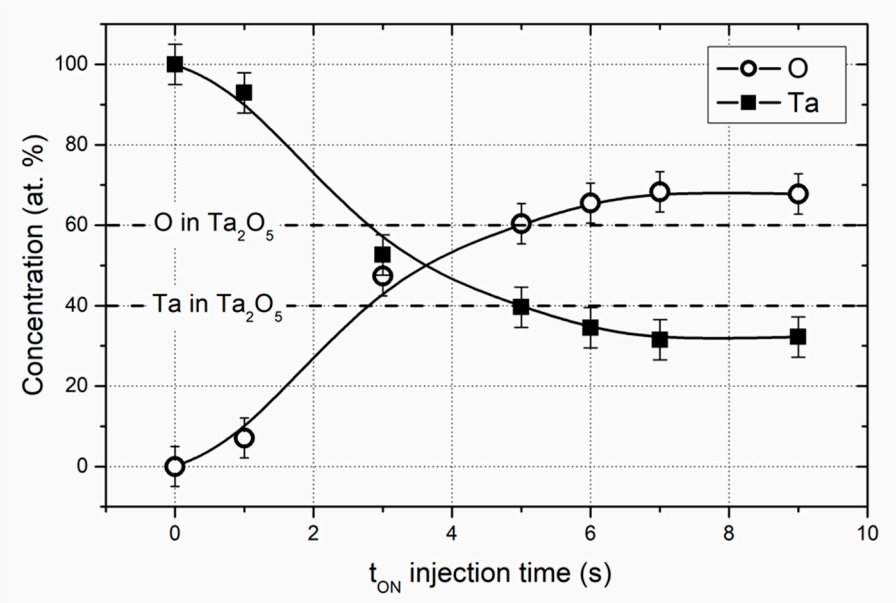

Figure 2. Tantalum and oxygen atomic concentrations as a function of the t_{ON} injection time. A continuous and reverse evolution is measured for both elements as t_{ON} rises. Solid lines are a guide for the eye. Horizontal dashed lines correspond to element concentrations of the stoichiometric Ta_2O_5 compound.

Both concentrations exhibit a continuous and gradual variation as t_{ON} rises. From the shortest t_{ON} of 1 s, the oxygen content reaches 7 at. % and increase rapidly up to 47% for t_{ON} = 3 s. A reverse evolution is clearly measured for the tantalum content with a symmetric drop of its concentration as the t_{ON} injection time rises. Nearly equivalent Ta and O concentrations are obtained when t_{ON} is around 3 s. Afterwards and for t_{ON} higher than 4 s, tantalum oxide films become oxygen-rich and both concentrations tend to stabilize to values corresponding to the stoichiometric Ta_2O_5 compound (dashed line in Figure 2). It is also worth noting that over-stoichiometric tantalum oxide thin films are prepared with t_{ON} injection times higher than 6 s and tending to a constant supply of oxygen. These oxygen-rich metal oxide compounds are often produced when the reactive sputtering process is fully set in the poisoned mode [37]. These operating conditions give rise to the formation of an oxide layer on the target surface, which is sputtered in an argon + oxygen atmosphere. As-deposited films are then all over-oxidized.

This symmetric, reverse and smooth evolution of metal and metalloid concentrations *vs.* t_{ON} injection time has ever been reported for other metal oxide thin films sputter-deposited by RGPP

Preprints (www.preprints.org) | NOT PEER-REVIEWED | Posted: 17 October 2023 doi:10.20944/preprints202310.1045.v1

playing only with the injection time of oxygen gas [38,39]. As t_{ON} increases, metal oxide (MeO_x) films become oxygen-rich, while the metal concentration symmetrically decreases. This correlates with an alternation of the sputtering mode from metallic to the oxidation one. These results chiefly prove and illustrate that RGPP is a valuable approach to precisely tune the chemical composition of MeO_x films (from sub- to over-stoichiometric compounds). This issue can be quite difficult to reach by conventional reactive sputtering (due to non-linear phenomena), and without implementing some feedback control systems or high pumping speed of the deposition chamber [40–42].

X-ray diffraction analyses of TaO_x films show that the crystalline structure is also influenced by the oxygen pulsing, particularly for t_{ON} injection times lower than 6 s (Figure 3). Without oxygen supply and as expected (not shown here), the typical pattern of a pure Ta film is obtained with diffracted signals corresponding to the bcc (body-centered cubic) α-phase. The shortest injection time of the oxygen gas (t_{ON} = 1 s) gives rise to weak and broad peaks. Most of them are related to the α-Ta ground state bcc structure with a crystal size of a few nanometers. It is interesting to notice the occurrence of two significant peaks at $2\theta = 34.80°$ and 64.51° assigned to (002) and (413) planes of the β-Ta metastable tetragonal structure, respectively. This metastable β-Ta phase has ever been reported for the deposition of Ta films by sputtering, particularly when impurities like residual oxygen are present during the deposition process [36,43–45]. These results can also be compared to the binary phase diagram of the Ta-O system [46]. The latter shows the co-existence of α- and β-phases for a wide range of concentrations (from 1 to 71 at. % of oxygen) and the occurrence of the β-phase for an oxygen concentration lower than 1 at. % at room temperature.

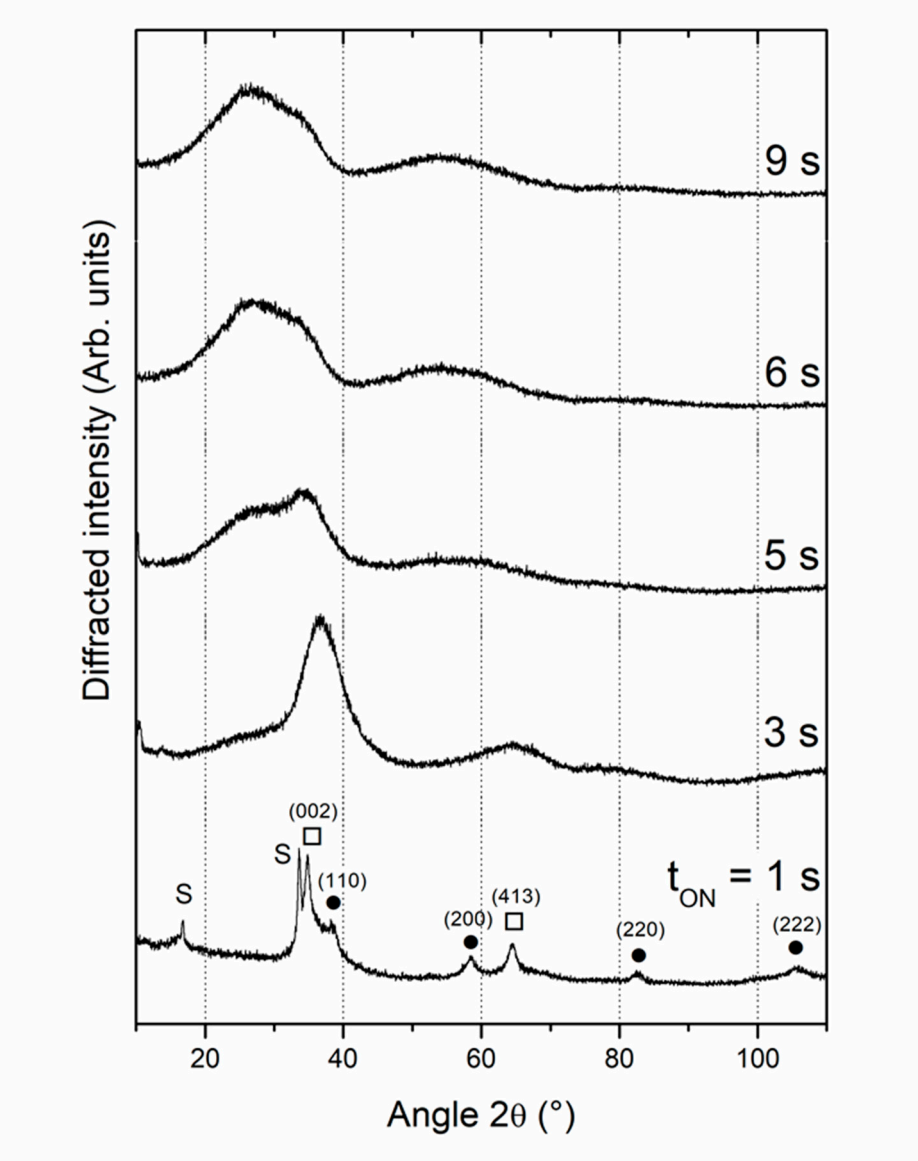

 doi:10.20944/preprints202310.1045.v1

Figure 3. X-ray diffraction patterns of TaO_x thin films prepared with various t_{ON} injection times. S = silicon substrate; ● = α-Ta ground state bcc structure; □ = β-Ta metastable tetragonal structure.

Colin *et al.* [47] pertinently showed that some mechanisms (stress, deposited energy) occurring during the early growth stages of Ta deposition favor the preferential nucleation of the β-Ta phase and its stabilization over the film thickness. They also demonstrated the key role of interface layer formation on the crystalline phase occurrence, with a major role of an amorphous Ta interlayer. For our tantalum oxide films prepared by RGPP with the shortest t_{ON} injection time, the t_{OFF} time is long enough to mainly keep the process in the elemental sputtering mode. As a result, the 1 s time of oxygen periodically supplied prevents the growth of the most stable α-Ta phase leading to an amorphization of the deposited film, and favoring the formation of the β-Ta phase. For these operating conditions, both α- and β-Ta phases coexist, and longer pulsing periods would promote the formation of the α-Ta phase [47].

Increasing more the t_{ON} injection time to 3 s induces even more an amorphous structure. Two broad signals around 35° and 65° are clearly recorded by XRD. They correspond to the range of 2θ angles related to α- and β-Ta phases, more accurately defined for t_{ON} = 1 s. This longer t_{ON} injection time prevents the process to remain mainly in the elemental sputtering mode. It rather extends it in the oxidized sputtering mode and an alternation between these two modes is then established. The long-range order of α- or β-Ta phase cannot be obtained to produce clear diffracted signals and an amorphous structure prevails. For t_{ON} injection times higher than 5 s, amorphization of the films is even more noticeable. The broad signal close to 2θ = 35° is shifted to lower angles and corresponds neither to the α- nor to the β-Ta phase. For films prepared with t_{ON} injection times higher than 6 s, XRD does not exhibit any diffracted signal, but the same broad envelop in-between 2θ = 20-40° and a weaker one close to 2θ = 55°. This type of patterns is typical of tantalum oxide thin films sputter-deposited at room temperature. These results well agree with former investigations previously published by others [48,49]. They are indicative of an amorphous structure of as-deposited Ta_2O_5 films on unheated substrates [50], or a possible nano-crystalline structure [51].

Chittinan *et al.* also deposited tantalum oxide films by reactive sputtering with the same strategy of oxygen pulsing [52]. In the same way, they produced films exhibiting an amorphous structure by conventional reactive sputtering or whatever their pulsing conditions. They recorded very similar X-ray diffraction patterns than those we obtained with t_{ON} injection times higher than 5 s, as shown in Figure 3.

Cross-section observations by scanning electron microscopy (SEM) show a poorly defined microstructure of tantalum oxide films sputter-deposited with various t_{ON} injection times (Figure 4). The typical columnar architecture of pure Ta films (not shown here) becomes less distinct even for the lowest t_{ON} of 1 s (Figure 4a). A brittle behavior is rather produced for films deposited with injection times lower than 6 s, where some fractures of the silicon wafer is extended from the substrate through the film thickness. This also means that tantalum oxide films present signs of a quite good adhesion to the silicon, despite the oxygen pulsing and deposition with no external heating of the substrate.

Preprints (www.preprints.org) | NOT PEER-REVIEWED | Posted: 17 October 2023 doi:10.20944/preprints202310.1045.v1

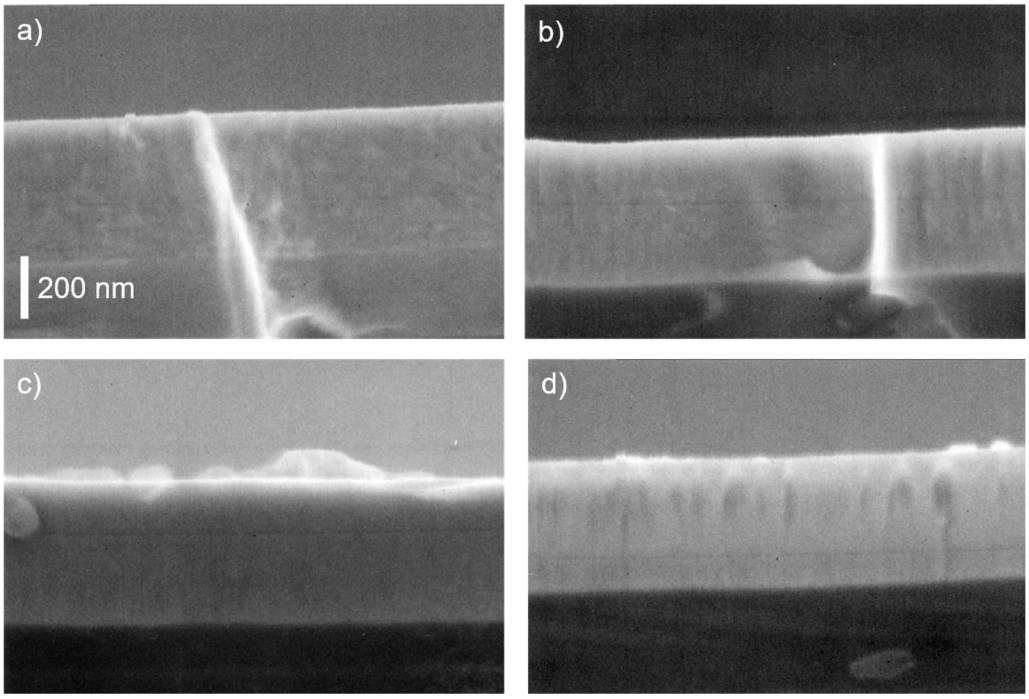

Figure 4. Cross-section pictures by SEM of tantalum oxide thin films sputter-deposited on Si substrates for different t_{ON} injection times: a) t_{ON} = 1 s, b) t_{ON} = 5 s, c) t_{ON} = 6 s, d) t_{ON} = 9 s.

For the longest t_{ON} injection times (e.g., t_{ON} = 9 s), a columnar growth becomes more distinguishable (Figure 4d). These pulsing conditions correspond to a nearly constant supply of the oxygen gas (reactive sputtering process mainly in oxidized mode). From composition analyses (Figure 2), the deposition of tantalum oxide films tends to the stoichiometric Ta_2O_5 compound. This cross-section microstructure agrees with Ito *et al.* results, who sputter-deposited tantalum pentoxide films at room temperature [53]. The authors similarly noticed a columnar structure corresponding to the first zone of structural zone models for films prepared at room temperature with density lower than that of the bulk Ta_2O_5 [54].

The poorly defined microstructure observed from SEM cross-sections (Figure 4) has been more precisely investigated by HRTEM observations and with a higher magnification. Two types of films can be prepared by adjusting the t_{ON} injection time: periodic multilayers or homogeneous tantalum oxide films (Figure 5). For t_{ON} = 3 s (Figure 5a and 5b), regular and nanometric Ta/TaO_x alternations are clearly produced with a period Λ = 3.4 nm through the total film thickness. The highest magnification (Figure 5b) shows that interfaces between metallic Ta (dark bands) and oxide TaO_x (bright bands) sub-layers are not frankly defined but gradually change. Despite very short times of oxygen gas supplies and stops (a few 10^2 ms are required to stabilize the pulsing signal at the beginning of t_{ON} and t_{OFF} times), oxygen species are not instantaneously evacuated for the sputtering chamber. In addition, oxygen diffusion from TaO_x to Ta sub-layers cannot be neglected leading to gradual and periodic variations of Ta and O concentrations through each sub-layer. However, the profile analysis (not shown here) clearly brings to the fore the nanometric period with metal and oxide alternations and a thickness λ_{Ta} = 1.9 nm (dark bands) and an oxide TaO_x sub-layer λ_{TaOx} = 1.5 nm (bright bands). Ta and O atomic concentrations performed by energy-dispersive X-ray spectroscopy reveal an oxygen-rich composition in the oxide sub-layer with 73±4 at. % of O and 27±4 at. % of Ta. These contents correspond to an oxide phase close to the Ta_2O_5 compound. A significant amount of oxygen is measured in metallic sub-layers with 10-19±4 at. % of O and 81-90±4 at. % of Ta, which is assigned to inclusion of oxygen in the Ta sub-layer. Even if a small probe size (1 nm) has been used for the EDX measurements, the presence of oxygen in the metallic sub-layers can also be explained by the widening of the electron beam crossing the specimen.

Preprints (www.preprints.org) | NOT PEER-REVIEWED | Posted: 17 October 2023 doi:10.20944/preprints202310.1045.v1

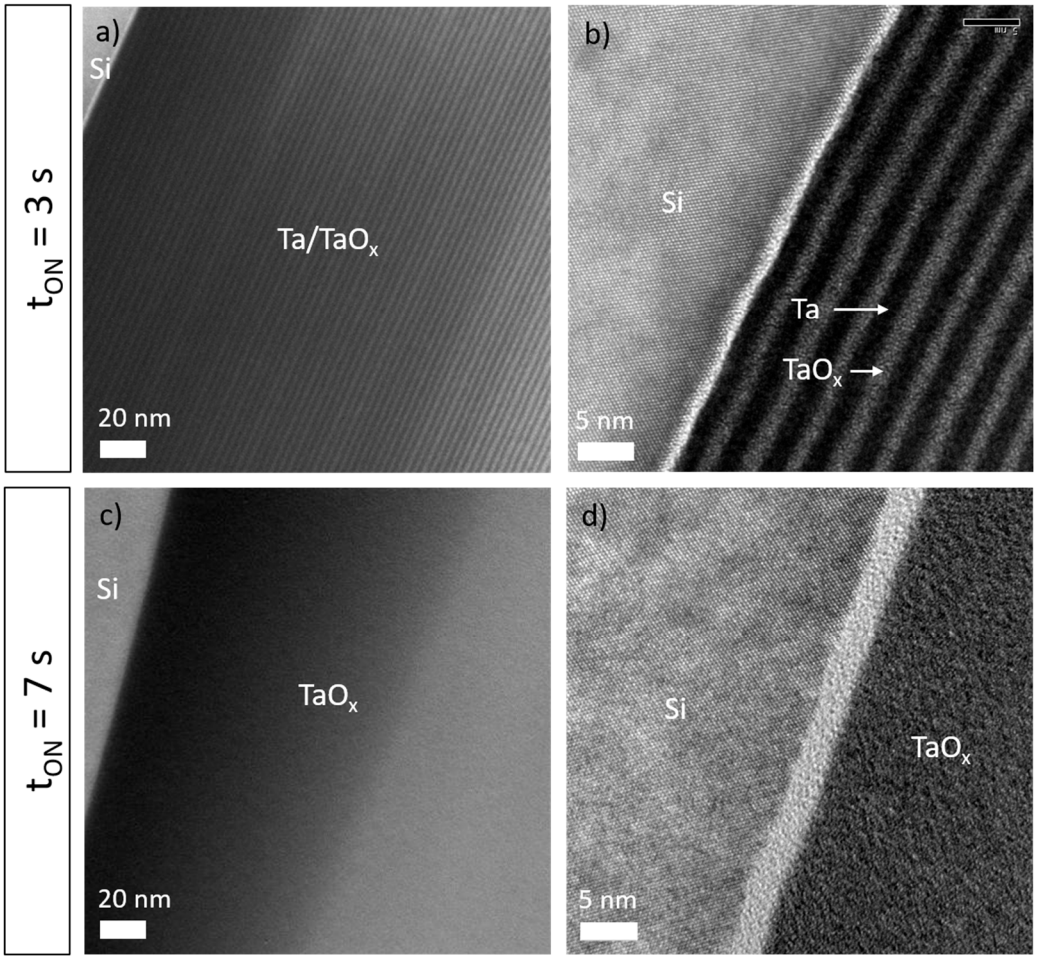

Figure 5. Cross-section views by HRTEM of tantalum oxide thin films sputter-deposited by RGPP using two different t_{ON} injection times: a) and b) t_{ON} = 3 s; c) and d) t_{ON} = 7 s. Periodic Ta/TaO$_x$ multilayers or homogeneous TaO$_x$ films can be prepared by means of a precise and single adjustment of the t_{ON} injection time.

It is also worth noting that high resolution images and diffraction patterns did not allow to detect any crystalline phase but amorphous Ta and TaO$_x$ sub-layers. A former study focused on Ta/TaO$_x$ multilayers with thicker periods showed that the metallic Ta sub-layer has to be higher than 10 nm to get nanometric crystal of the bcc α-Ta phase; the oxide TaO$_x$ sub-layer remaining amorphous whatever the thickness [48]. In our study, due to the very low thickness of sub-layers (lower than 2 nm), one can expect an amorphous structure of Ta and TaO$_x$ alternations. As a result, Ta/TaO$_x$ nanometric multilayers prepared with t_{ON} injection times lower than 5 s are completely amorphous and can be rather defined as a-Ta:O/a-Ta$_2$O$_5$ alternations. For t_{ON} injection times higher than 5 s, homogeneous and amorphous tantalum oxide thin films are obtained (Figure 5c and 5d). No alternations of bright and dark bands are observed for these pulsing conditions, but a rather dark grey shading with a random distribution of atoms, as shown in Figure 5d for the highest magnification. Ta and O concentrations are in the range 25-29±4 at. % and 71-75±4 at. %, respectively. These contents agree with the overall composition previously determined by EPMA and presented in Figure 2.

Similar Me/MeO$_x$, [55,56] Me/MeN$_y$, [57] MeN$_y$/MeO$_x$N$_y$ [58] periodic multilayers have ever been reported for other ceramic thin films prepared by reactive sputtering using RGPP but with thicker periods. Assuming deposition rates of the pure metal (process in elemental mode) and that of the corresponding compound (process in poisoned mode), and if the pulsing period is not too short with a suitable t_{ON} injection time, periodic alternations can be fabricated with a period thickness Λ of a few nanometers and with metal/compound interfaces in the order of the nanometer. However, the smallest metal/compound alternations also depend on the reactivity of the metalloid towards the

Preprints (www.preprints.org) | NOT PEER-REVIEWED | Posted: 17 October 2023 doi:10.20944/preprints202310.1045.v1

metal, especially when oxygen is involved with very reactive metals like titanium for instance. For such conditions, no clear multilayers can be reached and kinetics of the reactive sputtering process as well as reactivity of metal *vs.* metalloid both restrain the minimum period thickness and the quality of alternations and interfaces.

3.2. Optical and electrical properties

Since tantalum oxide is an attractive thin film material for optical applications, optical transmittance of the films deposited on glass substrate has been measured in the visible range and for various t_{ON} injection times (Figure 6).

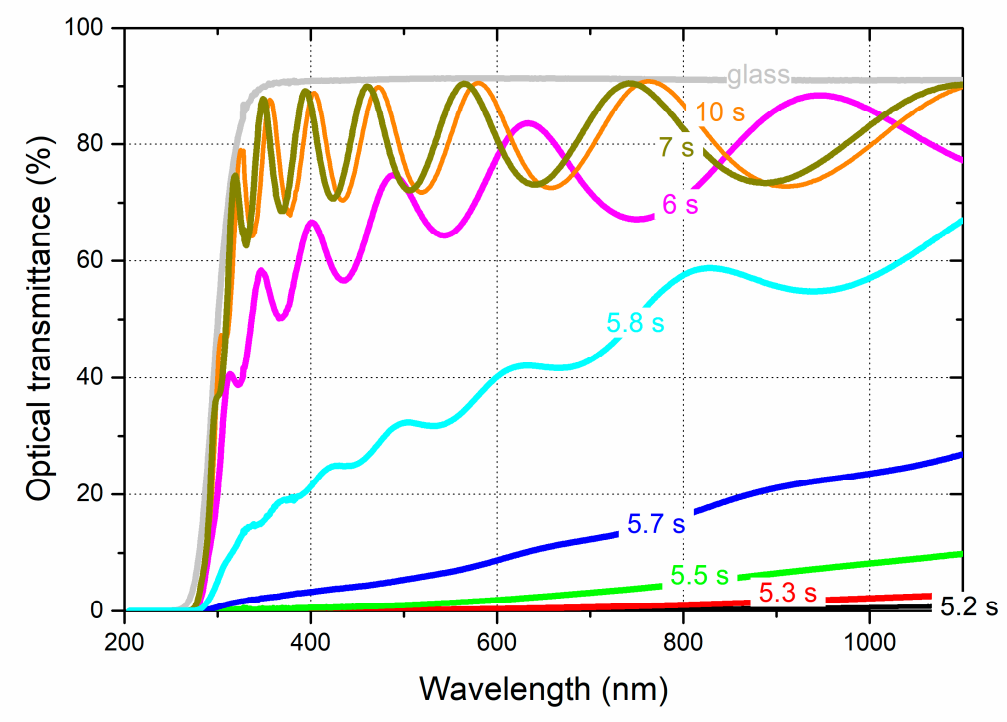

Figure 6. Optical transmittance spectra in the visible range of tantalum oxide thin films sputter-deposited on glass and for different t_{ON} injection times. For t_{ON} lower than 5 s, films are completely absorbent. Glass substrate is also shown as a reference.

For films prepared with t_{ON} lower than 5 s, no transmitted signal is measured for wavelengths in-between 200-1100 nm. Reactive gas supplied in the sputtering process is too short to incorporate enough oxygen in the film. Longer t_{ON} injection times (particularly from 5.3 to 5.8 s) lead to semi-transparent thin films with an optical transmittance of a few %, which gradually increases when wavelength tends to the infrared region. Some fringes start appearing for t_{ON} > 5.8 s but films prepared with such conditions still remains significantly absorbent with an optical transmittance lower than 70% at 1100 nm and progressively reducing for becoming null at 280 nm.

A further increase of the t_{ON} injection time leads to transparent tantalum oxide thin films (average transmittance higher than 80%) exhibiting typical interferential fringes. It is interesting to observe that from t_{ON} = 7 s and when oxygen injection tends to a constant supply, films show nearly the same optical transmittance. It well correlates with a stabilization of the chemical composition (O and Ta concentration become constant, as shown in Figure 2) and a homogeneous structure observed at the nanoscale from HRTEM (Figure 5c and 5d). The range of t_{ON} injection times included between 5 s and 7 s appears as the most interesting operating conditions to largely tune the optical transmittance of the films from absorbent to transparent in the visible region. In addition, such a range also corresponds to the maximum deposition rate formerly measured and discussed (Figure 1).

Absorption edge in the near UV region is also influenced by the oxygen supply with a blue shift as t_{ON} rises. This behavior has also been measured for other transparent metal oxide films prepared

 doi:10.20944/preprints202310.1045.v1

by reactive sputtering likewise pulsing the oxygen gas [39,59]. It is closely connected to oxygen vacancies in the film, which create states in the optical band gap, below the conduction band [60]. Increasing the t_{ON} injection time until a constant supply of oxygen reduces the density of oxygen deficiency in the film. Optical transparency in the visible range is favored and the band gap increases, which correlates with a slight shift of the absorption edge to lower wavelengths.

This gradual evolution of optical properties corroborates other investigations devoted to some metal oxide thin films prepared by RGPP [61]. Similarly, playing with a suitable range of t_{ON} injection times allows a wide tunability of many physical properties, not solely optical characteristics but electronic transport properties as well [62]. To that end, the electrical conductivity of tantalum oxide thin films prepared on glass and for different t_{ON} injection times was measured as a function of the temperature (Figure 7). Without oxygen injection (t_{ON} = 0 s), conductivity of pure Ta films is higher than 2.06×10^{6} S m^{-1} at 300 K and is slightly influenced by the temperature change. The evolution of resistivity *vs.* temperature (not shown here) gives rise to a typical metallic-like behavior with a temperature coefficient of resistance (TCR_{300K}) at room temperature of 1.16×10^{-3} K^{-1}. This value is lower than that of the bulk (TCR Ta bulk at 300 K = 3.54×10^{-3} K^{-1} [63]) as often reported for thin films and mainly assigned to the number of grain boundaries per electron mean free path in polycrystalline metallic thin films [64]. Increasing such a number, TCR reduces and can even change of sign (from positive to negative) although the conductivity is kept in a metallic regime.

Introducing the oxygen gas leads to more resistive films although the order of magnitude of conductivity is still in the metallic range up to t_{ON} = 4 s. Conductivity largely drops to a few 10^{5} S m^{-1}, but is inversely influenced by temperature even for the shortest t_{ON} = 1 s since films become slightly more conductive as the temperature rises. A negative TCR_{300K} is then obtained, which reduces from -2.20×10^{-4} to -2.66×10^{-4} K^{-1} when t_{ON} changes from 1 to 4 s, respectively. This loss of electrical conductivity with a negative TCR value has ever been measured for other metal oxide thin films containing a few at. % of oxygen or exhibiting a sub-stoichiometric composition [35,48,56]. These uncommon electronic transport behaviors are typical of disordered or poorly crystalline metal-rich oxide thin films, especially when Ta β-phase is produced [65]. It is worth noting that this range of t_{ON} injection times corresponds to Ta-rich oxide films (Figure 2) exhibiting a periodic multilayered nanostructure (Figure 5). In addition, films prepared with 1 s ≤ t_{ON} ≤ 4 s are optically absorbent (Figure 6) with a poorly crystalline structure composed of α-Ta, β-Ta and amorphous tantalum oxide phase mixture (Figure 3), which finally vanishes to produce a complete amorphous structure for longer t_{ON} injection times.

Preprints (www.preprints.org) | NOT PEER-REVIEWED | Posted: 17 October 2023 doi:10.20944/preprints202310.1045.v1

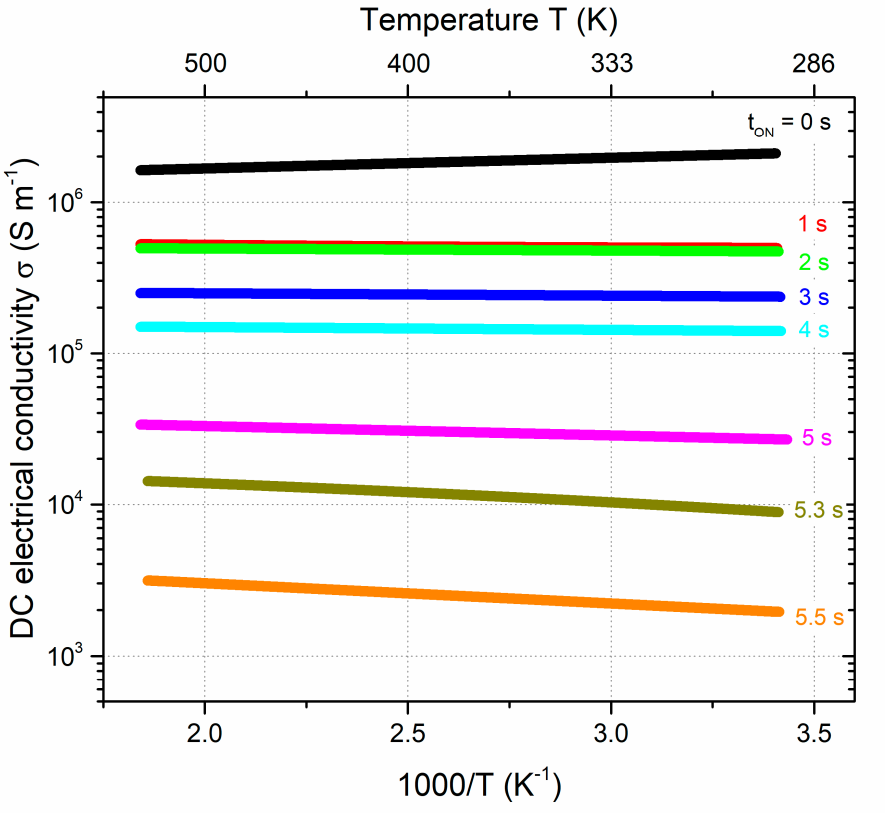

Figure 7. DC electrical conductivity as a function of the reciprocal of temperature 1000/T measured on tantalum oxide films prepared on glass substrate with t_{ON} injection times lower than 5.5 s (the corresponding temperature T is also indicated on the top axis).

Increasing more the t_{ON} injection time until a constant oxygen supply produces more resistive films and for t_{ON} higher than 5.5 s, conductivity cannot be measured with our system. For these deposition conditions, films become semi-conductors and lastly insulators. For films obtained with t_{ON} in-between 5-5.5 s, conductivity *vs.* reciprocal temperature (Arrhenius plot) gives rise to a clear linear evolution indicating a thermally activated conduction mechanism. The activation energy calculated for this range of t_{ON} injection times increases from 10 to 26 meV, which are quite low values compared to other oxide materials. These results well correlate with pulsing conditions corresponding to the deposition of oxygen-deficient Ta_2O_5 films. A short increase of the t_{ON} injection time leads to a fast oxygen-enrichment of the films and consequently, they rapidly exhibit dielectric characteristics (transparent in the visible region and insulator). Baker *et al.* [66] recently reported very similar results on tantalum oxide films prepared by changing the total chamber sputtering pressure. They also brought to the fore an abrupt increase of resistivity with an increasing oxygen content. They measured a gradual transition from metallic conduction to an activated tunneling through the oxide phase with an exponential relationship between oxygen concentration and activation energy for films tending to the Ta_2O_5 compound.

4. Conclusions

Tantalum oxide thin films 500 nm thick are sputter-deposited by DC reactive magnetron sputtering. A Ta target is sputtered in a reactive atmosphere composed of Ar and O_2 gases. The reactive gas pulsing process, namely RGPP, is implemented introducing the oxygen gas with a constant pulsing period T = 10 s while a systematic change of the t_{ON} injection time is performed. A reverse and gradual evolution of tantalum and oxygen concentrations is thus obtained as a function of an increasing t_{ON} injection time leading to an over-stoichiometric Ta_2O_5 compound when the oxygen supply tends to be constant (t_{ON} = T = 10 s). Deposition rate *vs.* t_{ON} reveals an unusual

maximum for intermediate t_{ON} injection times, which is mainly connected to the high sputtering yield of the Ta_2O_5 compound compared to that of the metal.

Whatever the oxygen supply, films exhibit a poorly defined columnar morphology with a brittle fracture observed from cross-section views. For the longest t_{ON} injection times, i.e., higher than 5 s, no long-range order is detected but an amorphous structure with a homogeneous and random distribution of atoms. These deposition conditions produce TaO_x films with an adjustable oxygen concentration from sub- to over-stoichiometric Ta_2O_5 compound. Such films also show a transparent optical transmittance in the visible region with typical interferential fringes and thus electrical properties corresponding to semiconducting characteristics with a thermally activated conductivity.

Playing with the t_{ON} injection time in-between 1-5 s allows the growth of periodic and nanometric Ta/TaO_x multilayers with a regular period length Λ of a few nanometers through the overall films thickness. For these pulsing conditions, both α- and β-Ta phases are obtained with a significant part of an amorphous oxide, which becomes predominant by increasing the t_{ON} injection time. Films exhibit a fully absorbent optical characteristic with a metallic-like electrical behavior. A precise adjustment of the t_{ON} injection time in the range of a few seconds leads to a change of sign (from positive to negative) of the temperature coefficient of resistance although the conductivity is maintained in a metallic regime.

These results clearly demonstrate that pulsing the introduction of the oxygen gas is a powerful tool for producing metal oxide thin films with structure exhibiting a homogeneous or a multilayered structure at the nanoscale with properties ranging from metal to semiconductor and finally insulator playing only with a single deposition parameter: the injection time of the reactive gas. In addition, the experimental strategy presented herein can be extended to other types of metal oxide systems or other nitride, carbide, sulfide compounds, and thus to gain insight into growth mechanisms that determine the final nanostructure of films sputter-deposited by RGPP.

Author Contributions: Conceptualization, data curation, writing—review and editing, funding acquisition, N. Martin.; Methodology, software, formal analysis, validation, J.M. Cote; Writing—review and editing, validation, J. Gavoille; Data curation, writing—review and editing, funding acquisition, V. Potin. All authors have read and agreed to the published version of the manuscript.

Funding: This research was partially funded by Fonds Européen de Développement Régional – FEDER, grant number CTE 6059 in the framework of the TOOLEXPERT Interreg V project.

Institutional Review Board Statement: Not applicable.

Informed Consent Statement: Not applicable.

Data Availability Statement: All data are presented in the current manuscript.

Acknowledgments: This work has been supported by the Région Bourgogne Franche-Comté and by EIPHI Graduate School (Contract 'ANR-17-EURE-0002').

Conflicts of Interest: The authors declare no conflict of interest. The funders had no role in the design of the study; in the collection, analyses, or interpretation of data; in the writing of the manuscript; or in the decision to publish the results.

References

1. Kim, H.J.; Park, K.; Kim, H.J. High-performance vacuum-processes metal oxide thin-film transistors: A review of recent developments. *J. Soc. Inf. Display* **2020**, 28, 591-622. https://doi.org/10.1002/jsid.886
2. Chen, R.; Lan, L. Solution-processed metal-oxide thin-film transistors: A review of recent developments. *Nanotechnol*ogy **2019**, 30, 312001-35. https://doi.org/10.1088/1361-6528/ab1860
3. Barsan, N.; Koziej, D.; Weimar, U. Metal oxide-based gas sensor research: How to? *Sens. Actuator. B-Chem.* **2007**, 121, 18-35. https://doi.org/10.1016/j.snb.2006.09.047
4. Granqvist, C.G. Transparent conductive electrodes for electrochromic devices: A review. *Appl. Phys. A* **1993**, 57, 19-24. https://doi.org/10.1007/bf00331211
5. Kim, J.S.; Kim, B.; Kim, H.; Kang, K. Recent progress on multimetal oxide catalysts for the oxygen evolution reaction. *Adv. Energy Mater.* **2018**, 8, 1702774-26. https://doi.org/10.1002/aenm.201702774

6. Losego, M.D.; Efremenko, A.Y.; Rhodes, C.L.; Cerruti, M.G.; Franzen, S.; Maria, J.P. Conductive oxide thin films: Model systems for understanding and controlling surface plasmon resonance. *J. Appl. Phys.* **2009**, 106, 024903-8. https://doi.org/10.1063/1.3174440
7. Chittinan, D.; Buranasiri, P.; Lertvanithphol, T.; Eiamchai, P.; Tantiwanichapan, K.; Sathukarn, A.; Limwichean, S.; Klamchuen, A.; Wutikhun, T.; Limsuwan, P., Nakajima, H.; Phae-ngam, W.; Triamnak, N.; Horprathum, M. Tailoring the structural and optical properties of fabricated TiO_2 thin films by O_2 duty cycle in reactive gas-timing magnetron sputtering. *Vacuum* **2023**, 214, 112205-11. https://doi.org/10.1016/j.vacuum.2023.112205
8. Medvedeva, J.E.; Buchholz, D.B.; Chang, R.P.H. Recent advances in understanding the structure and properties of amorphous oxide semiconductors. *Adv. Electron. Mater.* **2017**, 3, 1700082-17. https://doi.org/10.1002/aelm.201700082
9. Moreira, H.; Costa-Barbosa, A.; Mariana Marques, S.; Sampaio, P.; Carvalho, S. Evaluation of cell activation promoted by tantalum and tantalum oxide coatings deposited by reactive DC magnetron sputtering. *Surf. Coat. Technol.* **2017**, 330, 260-269. https://doi.org/10.1016/j.surfcoat.2017.10.019
10. Sharath, S.U.; Joseph, M.J.; Vogel, S.; Hildebrandt, E.; Komissinskiy, P.; Kurian, J.; Schroeder, T.; Alff, L. Impact of oxygen stoichiometry on electroforming and multiple switching modes in TiN/TaO_x/Pt based ReRAM. *Appl. Phys. Lett.* **2016**, 109, 173503-4. ttps://doi.org/10.1063/1.4965872
11. Franke, E.; Schubert, M.; Trimble, C.L.; Devries, M.J.; Woollam, J.A. Optical properties of amorphous and polycrystalline tantalum oxide measured by spectroscopic ellipsometry. *Thin Solid Films* **2001**, 388, 283-289. https://doi.org/10.1016/s0040-6090(00)01881-2
12. Kazuki, T.; Yasusei, Y.; Shanhu, B.; Masahisa, O.; Kazuki, Y. Solid electrolyte of tantalum oxide thin film deposited by reactive DC and RF magnetron sputtering for all-solid-state switchable mirror glass. *Sol. Energy Mater. Sol. Cells* **2008**, 92, 120-125. https://doi.org/10.1016/j.solmat.2007.01.022
13. Borisenko, V.E.; Parkhutik, V.P. RBS study of transient thermal anodic oxidation of tantalum films. *Phys. Status Solidi A-Appl. Mat.* **1986**, 93, 123-130. https://doi.org/10.1002/pssa.2210930116
14. Gangloff, D.; Shi, M.; Wu, T.; Bylinskii, A.; Braverman, B.; Gutierrez, M.; Nichols, R.; Li, J.; Aichholz, K.; Cetina, M. Karpa, L.; Jelenkovic, B.; Chuang, I.; Vuletic, V. Preventing and reversing vacuum-induced optical losses in high-finesse tantalum (V) oxide mirror coatings. *Opt. Express* **2015**, *23*, 18014-18028. https://doi.org/10.1364/oe.23.018014
15. Yun, S.N.; Wang, L.; Guo, W.; Ma, T.L. Non-Pt counter electrode catalysts using tantalum oxide for low-cost dye-sensitized solar cells. *Electrochem. Commun.* **2012**, 24, 69-73. https://doi.org/10.1016/j.elecom.2012.08.008
16. Schmitt, K.; Oehse, K.; Sulz, G.; Hoffmann, C. Evanescent field sensors based on tantalum pentoxide waveguides – A review. *Sensors*, **2007**, 8, 711-738. https://doi.org/10.3390/s8020711
17. Rouahi, A.; Challali, F.; Dakhlaoui, I.; Vallee, C.; Salimy, S.; Jomni, F.; Yangui, B.; Besland, M.P.; Goullet, A.; Sylvestre, A. Structural and dielectric characterization of sputtered tantalum titanium oxide thin films for high temperature capacitor applications. *Thin Solid Films*, **2016**, 606, 127-132. https://doi.org/10.1016/j.tsf.2016.03.047
18. Kimura, H.; Mizuki, K.; Kamiyama, S.; Suzuki, H. Extended X-ray absorption fine-structure analysis of the difference in local-structure of tantalum oxide capacitor films produced by various annealing methods. *Appl. Phys. Lett.* **1995**, 66, 2209-221. https://doi.org/10.1063/1.113169
19. Lau, W.S.; Tan, T.S.; Babu, P.; Sandler, N.P. Mechanism of leakage current reduction of tantalum oxide capacitors by titanium doping. *Appl. Phys. Lett.* **2007**, 90, 112903-3. https://doi.org/10.1063/1.2710000
20. Yu, H.B.; Zhu, S.Y.; Yang, X.; Wang, X.H.; Sun, H.W.; Huo, M.X. Synthesis of coral-like tantalum oxide films via anodization in mixed organic-inorganic electrolytes. *PLoS One* **2013**, 8, e66447-6. https://doi.org/10.1371/journal.pone.0066447
21. Ohno, T.; Samukawa, S. Resistive switching in a few nanometers thick tantalum oxide thin film formed by a metal oxidation. *Appl. Phys. Lett.* **2015**, 106, 173110-4. https://doi.org/10.1063/1.4919724
22. He, X.M.; Wu, J.H.; Zhao, L.L.; Mang, J.; Gao, X.D.; Li, X.M. Synthesis and optical properties of tantalum oxide films prepared by ionized plasma-assisted pulsed laser deposition. *Solid State. Commun.* **2008**, 147, 90-93. https://doi.org/10.1016/j.ssc.2008.05.007
23. Kim, I.; Ahn, S.D.; Cho, B.W.; Ahn, S.T.; Lee, J.Y.; Chun, J.S.; Lee, W.J. Microstructure and electrical properties of tantalum oxide thin film prepared by electron cyclotron resonance plasma enhanced chemical vapor deposition. *Jpn. J. Appl. Phys.* **1994**, 33, 6691-6698. https://doi.org/10.1143/jjap.33.6691

24. Rahmati, B.; Sarhan, A.A.D.; Zalnezhad, E.; Kamiab, Z.; Dabbagh, A.; Choudhury, D.; Abas, W.A.B.W. Development of tantalum oxide (Ta-O) thin film coating on biomedical Ti-6Al-4V alloy to enhance mechanical properties and biocompatibility. *Ceram. Int.* **2016**, 42, 466-480. https://doi.org/10.1016/j.ceramint.2015.08.133
25. Wang, S.C.; Liu, K.Y., Huang, J.L. Tantalum oxide film prepared by reactive magnetron sputtering deposition for all-solid-state electrochromic device. *Thin Solid Films* **2011**, 520, 1454-1459. https://doi.org/10.1016/j.tsf.2011.08.046
26. Ngaruiya, J.M., Venkataraj, S.; Drese, R.; Kappertz, O.; Leervad Pedersen, T.P.; Wuttig, M. Preparation and characterization of tantalum oxide films produced by reactive DC magnetron sputtering. *Phys. Stat. Sol.* **2003**, 198, 99-110. https://doi.org/10.1002/pssa.200306444
27. Depla, D. De Gryse, R. Target poisoning during reactive magnetron sputtering: Part I: The influence of ion implantation. *Surf. Coat. Technol.* **2004**, 183, 184-189. https://doi.org/10.1016/j.surfcoat.2003.10.006
28. Berg, S.; Särhammar, E.; Nyberg, T. Upgrading the "Berg-model" for reactive sputtering processes. *Thin Solid Films* **2014**, 565, 186-192. https://doi.org/10.1016/j.tsf.2014.02.063
29. Billard, A.; Frantz, C. Attempted modelling of thickness and chemical heterogeneity in coatings prepared by dc reactive magnetron sputtering. *Surf. Coat. Technol.* **1993**, 59, 41-47. https://doi.org/10.1016/0257-8972(93)90052-p
30. Martin, N.; J. Lintymer, J.; Gavoille, J.; Chappé, J.M.; Sthal, F.; Takadoum, J.; Vaz, F.; Rebouta, L. Reactive sputtering of TiO_xN_y coatings by the reactive gas pulsing process – Part II : the role of the duty cycle. *Surf. Coat. Technol.* **2007**, 201, 7727-7732. https://doi.org/10.1016/j.surfcoat.2007.03.021
31. Martin, N.; Sanjinès, R.; Takadoum, J.; Lévy, F. Enhanced sputtering of titanium oxide, nitride and oxynitride thin films by the reactive gas pulsing technique. *Surf. Coat. Technol.* **2007**, 142-144, 615-620. https://doi.org/10.1016/s0257-8972(01)01149-5
32. Petitjean, C.; Rousselot, C.; Pierson, J.F.; Billard, A. Reactive sputtering of iron in Ar-N_2 and Ar-O_2 mixtures. *Surf. Coat. Technol.* **2005**, 200, 431-434. https://doi.org/10.1016/j.surfcoat.2005.02.028
33. Martin, N.; Bally, A.R.; Hones, P.; Sanjinès, R.; Lévy, F. High rate and process control of reactive sputtering by reactive gas pulsing : the Ti - O system. *Thin Solid Films* **2000**, 377-378, 550-556. https://doi.org/10.1016/s0040-6090(00)01440-1
34. Khemasiri, N., Chananonnawathorn, C.; Klamchuen, A.; Jessadaluk, S.; Pankiew, A.; Vuttivong, S.; Eiamchai, P.; Horprathum, M.; Pornthreeraphat, S.; Kasamechonchung, P.; Tantisantisom, K.; Boonkoom, T.; Songsiririthigul, P.; Nakajima, H.; Nukeaw, J. Crucial role of reactive pulse-gas on a sputtered Zn_3N_2 thin film formation. *RSC Adv.* **2016**, 6, 94905-94910. https://doi.org/10.1039/c6ra09972f
35. Xu, X.; M. Arab Pour Yazdi, M.; Salut, R.; Cote, J.M.; Billard, A.; Martin, N. Structure, composition and electronic transport properties of tungsten oxide thin films sputter-deposited by the reactive gas pulsing process. *Mater. Chem. Phys.* **2018** 205, 391-400. https://doi.org/10.1016/j.matchemphys.2017.11.048
36. Oechsner, H.; Schoof, H.; Stumpe, E. Sputtering of Ta_2O_5 by Ar^+ ions at energies below 1 keV. *Surf. Sci.* **1978** 76, 343-354. https://doi.org/10.1016/0039-6028(78)90102-4
37. Rousselot, C.; Martin, N. Hysteresis effect in DC and RF reactive magnetron sputtering. *Vide-Sci. Technol. Appl.* **1999**, 54, 481-490.
38. Djeffal, F.; Martin, N., Ferhati, H.; Benhaya, A. Tunable band-selective photodetector based on sputter-deposited SnO_x thin-films: Effect of reactive gas pulsing process. *J. Alloy. Compd.* **2023**, 968, 171851-8. https://doi.org/10.1016/j.jallcom.2023.171851
39. Xu, X.; Arab Pour Yazdi, M.; Salut, R.; Cote, J.M.; Billard, A.; Martin, N. Structure, composition and electronic transport properties of tungsten oxide thin film sputter-deposited by the reactive gas pulsing process. *Mater. Chem. Phys.* **2018**, 205, 391-400. https://doi.org/10.1016/j.matchemphys.2017.11.048
40. Sproul, W.D. High-rate reactive sputtering process-control. *Surf. Coat. Technol.* **1987**, 33, 73-81. https://doi.org/10.1016/0257-8972(87)90178-2
41. Hmiel, A.F. Partial-pressure control of reactively sputtered titanium nitride. *J. Vac. Sci. Technol.* **1985**, A3, 592-595. https://doi.org/10.1116/1.572957
42. Larsson, T.; Blom, H.O.; Nender, C.; Berg, S. A physical model for eliminating instabilities in reactive sputtering. *J. Vac. Sci. Technol.* **1988**, A6, 1832-1836. https://doi.org/10.1116/1.575264
43. Baker, P.N. Preparation and properties of tantalum thin films. *Thin Solid Films* **1972**, 14, 3-25. https://doi.org/10.1016/0040-6090(72)90365-3

44. Knepper, R., Stevens, B., Baker, S.P. Effect of oxygen on the thermomechanical behavior of tantalum thin films during the β-α phase formation. *J. App. Phys.* **2006**, 100, 123508. https://doi.org/10.1063/1.2388742
45. Feinstein, L.G., Huttemann, R.D. Factors controlling the structure of sputtered Ta films. *Thin Solid Films* **1973**, 16, 129-145. https://doi.org/10.1016/0040-6090(73)90163-6
46. Garg, S.P.; Krishnamurty, N.; Awasthi, A.; Venkatraman, M. The Ta-O (Oxygen-Tantalum) system. *J. Phase Equilib.* **1996**, 17, 63-77. https://doi.org/10.1007/bf02648373
47. Colin, J.J.; Abadias, G.; Michel, A.; Jaouen, C. On the origin of the metastable β-Ta phase in tantalum sputtered thin films. *Acta Mater.* **2017**, 126, 481-493. https://doi.org/10.1016/j.actamat.2016.12.030
48. Cacucci, A.; Loffredo, S.; Potin, V.; Imhoff, L.; Martin, N. Interdependence of structural and electrical properties in tantalum/tantalum oxide multilayers. *Surf. Coat. Technol.* **2013**, 227, 38-41. https://doi.org/10.1016/j.surfcoat.2012.10.064
49. Zhou, J.C.; Luo, D.T.; Li, Y.Z., Liu, Z. Effect of sputtering pressure and rapid thermal annealing on optical properties of Ta_2O_5 thin films. *Trans. Nonferrous Met. Soc. China* **2009**, 19, 359-363. https://doi.org/10.1016/s1003-6326(08)60278-2
50. Vlcek, J.; Rezek, J.; Houska, J.; Cerstvy, R.; Bugyi, R. Process stabilization and a significant enhancement of the deposition rate in reactive high-power impulse magnetron sputtering of ZrO_2 and Ta_2O_5 films. *Surf. Coat. Technol.* **2013**, 236, 550-556. https://doi.org/10.1016/j.surfcoat.2013.10.052
51. Ngaruiya, J.; Venkataraj, S.; Drese, R.; Kappertz, O.; Leervad Perdersen, T.P.; Wuttig, M. Preparation and characterization of tantalum oxide thin films produced by reactive DC magnetron sputtering. *Phys. Stat. Sol.* **2003**, 198, 99-110. https://doi.org/10.1002/pssa.200306444
52. Chittinan, D.; Buranasiri, P.; Lertvanithphol, T.; Eiamchai, P.; Patthanasettakul, V.; Chananonnawathorn, C.; Limwichean, S.; Nuntawong, N.; Klamchuen, A.; Muthitamongkol, P.; Limsuwan, P.; Chindaudom, P.; Nukeaw, J.; Nakajima, H., Horprathum, M. Observations of the initial stage on reactive gas-timing sputtered TaO thin films by dynamic in situ spectroscopic ellipsometry. *Optic. Mater.* **2019**, 92, 223-232. https://doi.org/10.1016/j.optmat.2019.04.040
53. Ito, Y.; Abe, Y.; Kawamura, M.; Kim, K.H.; Kiba, T. Influence of substrate cooling on ion conductivity of tantalum oxide thin films prepared by reactive sputtering using water vapor injection. *Thin Solid Films* **2020**, 710, 138276-5. https://doi.org/10.1016/j.tsf.2020.138276
54. Thornton, J.A. Influence of apparatus geometry and deposition conditions on the structure and topography of thick sputtered coatings. *J. Vac. Sci. Technol.* **1974**, 11, 666-670. https://doi.org/10.1116/1.1312732
55. Parreira, N.; Polcar, T. Cavaleiro, A. Characterization of W-O coatings deposited by magnetron sputtering with reactive gas pulsing. *Surf. Coat. Technol.* **2007**, 201, 5481-86. https://doi.org/10.1016/j.surfcoat.2006.07.017
56. Potin, V.; Cacucci, A.; Martin, N. Correlations between structure, composition and electrical properties of tungsten/tungsten oxide periodic multilayers sputter deposited by gas pulsing. *Superlattices Microstruct.* **2017**, 101, 127-137. https://doi.org/10.1016/j.spmi.2016.10.071
57. El Mouatassim, A.; Pac, M.J.; Pailloux, F.; Amiard, G.; Henry, P.; Rousselot, C.; Eyidi, D.; Tuilier, M.H.; Cabioc'h, T. On the possibility of synthesizing multilayered coatings in the (Ti, Al)N system by RGPP: A microstructural study. *Surf . Coat. Technol.* **2019**, 374, 845-851. https://doi.org/10.1016/j.surfcoat.2019.06.071
58. Fenker, M.; Kappl, H., Sandu, C.S. Precise control of multilayered structures of Nb-O-N thin films by the use of reactive gas pulsing process in DC magnetron sputtering. *Surf. Coat. Technol.* **2008**, 202, 2358-2362. https://doi.org/10.1016/j.surfcoat.2007.08.007
59. Springer, S.G.; Schmid, P.E.; Sanjinès, R.; Lévy, F. Morphology and electrical properties of titanium oxide nanometric multilayers deposited by DC reactive sputtering. *Surf. Coat. Technol.* **2002**, 151-152, 51-54. https://doi.org/10.1016/s0257-8972(01)01584-5
60. Li, J.; Liu, W.; Wei, Y.; Yan, Y. Effect of oxygen content on the properties of sputtered TaOx electrolyte film in all-solid-state electrochromic devices. *Coatings* **2022**, 12, 183-15. https://doi.org/10.3390/coatings12121831
61. Martin, N.; Besnard, A.; Sthal, F.; Takadoum, J. The reactive gas pulsing process for tuneable properties of sputter deposited titanium oxide, nitride and oxynitride coatings. *Inter. J. Mater. Prod. Technol.* **2010**, 39, 159-177. https://doi.org/10.1504/ijmpt.2010.034268
62. Cacucci, A.; Tsiouassis, I., Potin, V.; Imhoff, L.; Martin, N.; Nyberg, T. The interdependence of structural and electrical properties in TiO_2/TiO/Ti periodic multilayers. *Acta Mater.* **2013**, 61, 4215-4225. https://doi.org/10.1016/j.actamat.2013.03.047

63. Desal, P.D.; Chu, T.K.; James, H.M.; Ho, C.Y. Electrical resistivity of selected elements. *J. Phys. Chem. Ref. Data* **1984**, 13, 1069-1096. https://doi.org/10.1063/1.555723
64. Reiss, G.; Vancea, J.; Hoffman, H. Grain-boundary resistance in polycrystalline metals. *Phys. Rev. Lett.* **1986**, 56, 2100-2103. https://doi.org/10.1103/physrevlett.56.2100
65. Schwartz, N.; Reed, W.A.; Polash, P.; Read, M.H. Temperature coefficient of resistance of beta-tantalum films and mixtures with b.c.c.-tantalum. *Thin Solid Films* **1972**, 14, 333-347. https://doi.org/10.1016/0040-6090(72)90433-6
66. Baker, A.; Engwall, A.M.; Bayu-Aji, L.B.; Bae, J.H.; Shin, S.J.; Moody, J.D.; Kucheyev, S.O. Tantalum suboxide films with tunable composition and electrical resistivity deposited by reactive magnetron sputtering. *Coatings* **2022**, 12, 917-10. https://doi.org/10.3390/coatings12070917